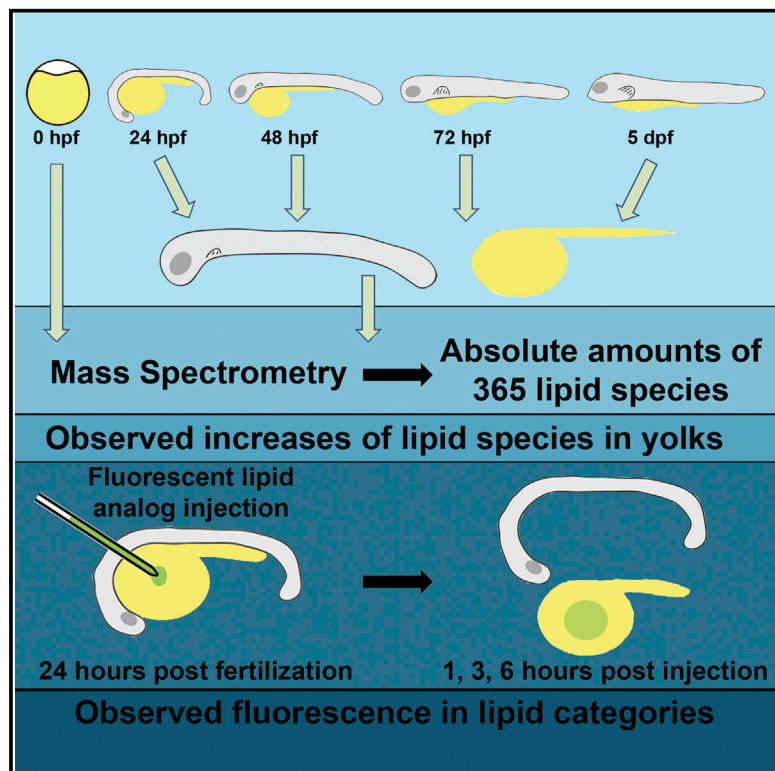# Zebrafish Embryonic Lipidomic Analysis Reveals that the Yolk Cell Is Metabolically Active in Processing Lipid

Graphical Abstract

Authors

Daniel Fraher, Andrew Sanigorski, Natalie A. Mellett, Peter J. Meikle, Andrew J. Sinclair, Yann Gibert

Correspondence

andrew.sinclair@deakin.edu.au (A.J.S.), y.gibert@deakin.edu.au (Y.G.)

In Brief

Fraher et al. develop a method to identify lipids separately in the zebrafish yolk and the embryonic body. Lipid usage and content are dynamic in the yolk and embryo during development. The yolk actively processes lipids prior to migration to the body during early embryogenesis.

Highlights

- Lipidomic analysis reveals lipid usage during early development

- Several lipids increase in concentration in the yolk sac during development

- Inhibition of PPARγ activity changes lipid profile during zebrafish embryogenesis

- Lipids are actively processed in the yolk during embryogenesis

CrossMark

CellPress

Zebrafish Embryonic Lipidomic Analysis Reveals that the Yolk Cell Is Metabolically Active in Processing Lipid

Daniel Fraher,[1] Andrew Sanigorski,[1] Natalie A. Mellett,[2] Peter J. Meikle,[2] Andrew J. Sinclair,[1,*] and Yann Gibert[1,*]

[1]Metabolic Genetic Diseases Laboratory, Metabolic Research Unit, Deakin University School of Medicine, 75 Pigdons Road, Geelong, VIC 3216, Australia
[2]Baker IDI Heart and Diabetes Institute, 75 Commercial Road, Melbourne, VIC 3004, Australia
*Correspondence: andrew.sinclair@deakin.edu.au (A.J.S.), y.gibert@deakin.edu.au (Y.G.)
http://dx.doi.org/10.1016/j.celrep.2016.01.016

SUMMARY

The role of lipids in providing energy and structural cellular components during vertebrate development is poorly understood. To elucidate these roles further, we visualized lipid deposition and examined expression of key lipid-regulating genes during zebrafish embryogenesis. We also conducted a semi-quantitative analysis of lipidomic composition using liquid chromatography (LC)-mass spectrometry. Finally, we analyzed processing of boron-dipyrromethene (BODIPY) lipid analogs injected into the yolk using thin layer chromatography. Our data reveal that the most abundant lipids in the embryo are cholesterol, phosphatidylcholine, and triglyceride. Moreover, we demonstrate that lipids are processed within the yolk prior to mobilization to the embryonic body. Our data identify a metabolically active yolk and body resulting in a dynamic lipid composition. This provides a foundation for studying lipid biology during normal or pharmacologically compromised embryogenesis.

INTRODUCTION

Lipids have significant roles in energy homeostasis, cellular structures, and cellular signaling (Belkhou et al., 1991; Simons and Ikonen, 1997; Spiegel et al., 1996). However, little is known about the influence of lipid composition on vertebrate embryogenesis and development. Many animals, known as lecitho-trophs, rely on maternally provided yolk for the nutrients and energy needed for embryonic growth (Allen and Pernet, 2007). Previous studies have established that maternally deposited lipids within the yolk provide an energy source for the developing organism and therefore considered the yolk as a nutrient reserve without metabolic activity (Heras et al., 2000; Hölttä-Vuori et al., 2010; Rosa et al., 2005). Based on this, essential fatty acids and other essential nutrients such as choline needed for structural development were thought to be stored within the yolk cell and mobilized when required (Wiegand, 1996). Individual vertebrate

oocytes and embryos have had their lipid content analyzed at a single time point (Ferreira et al., 2010; González-Serrano et al., 2013); the dynamics of lipid content were not studied during development. A recent study by Guan et al. (2013) examined the lipid profile of the fruit fly, *Drosophila melanogaster*, during embryonic, pupal, larval, and adult stages. While this study provided insight into lipid requirements, triglyceride usage, and changes in sphingolipids during fruit fly development, the focus of their study was membrane lipids in a non-vertebrate animal, and the authors were unable to discriminate between the yolk lipid reserve and lipids present in the body of the embryo (Guan et al., 2013). Cumulatively, these studies have provided a broad picture of the roles of lipids and their importance during development, but a comprehensive understanding of the complex remodeling of lipids within vertebrate development requires further study.

The zebrafish (*Danio rerio*) is a vertebrate model organism that has been intensively used to study developmental biology and human diseases (Dawid, 2004; Zon, 1999). Recently, zebrafish have been used to study various aspects of lipid biology including lipid metabolism, the genes regulating lipid processing, and the roles of lipids in diseases (Carten et al., 2011; Flynn et al., 2009; Schlegel and Stainier, 2006). Importantly, many properties of lipid biology present in zebrafish are conserved in humans. Homologous genes regulating lipid metabolism are found in zebrafish and they share a similar lipid and lipoprotein metabolism to that of humans (Miyares et al., 2014; Schlegel and Gut, 2015; Schlegel and Stainier, 2006; Thisse et al., 2001; Thisse and Thisse, 2004). This homology has allowed researchers unprecedented insight into disease pathology including atherosclerosis, non-alcoholic fatty-liver disease, and obesity (Fang et al., 2014; Flynn et al., 2009; Schlegel, 2012).

The zebrafish is a lecithotrophic organism (discussed in Kunz-Ramsay, 2013), relying on a yolk contents for nutrition throughout development until an early larval stage, at ~5 days post fertilization (dpf), when it can commence feeding. Because of this reliance on a yolk, zebrafish embryos can be considered a "closed system," meaning that their nutrient intake is uninfluenced by outside factors. Therefore, potential experimental variables due to feeding can be eliminated during embryogenesis. The zebrafish is amenable to a variety of techniques for studying metabolism during development including pharmacological
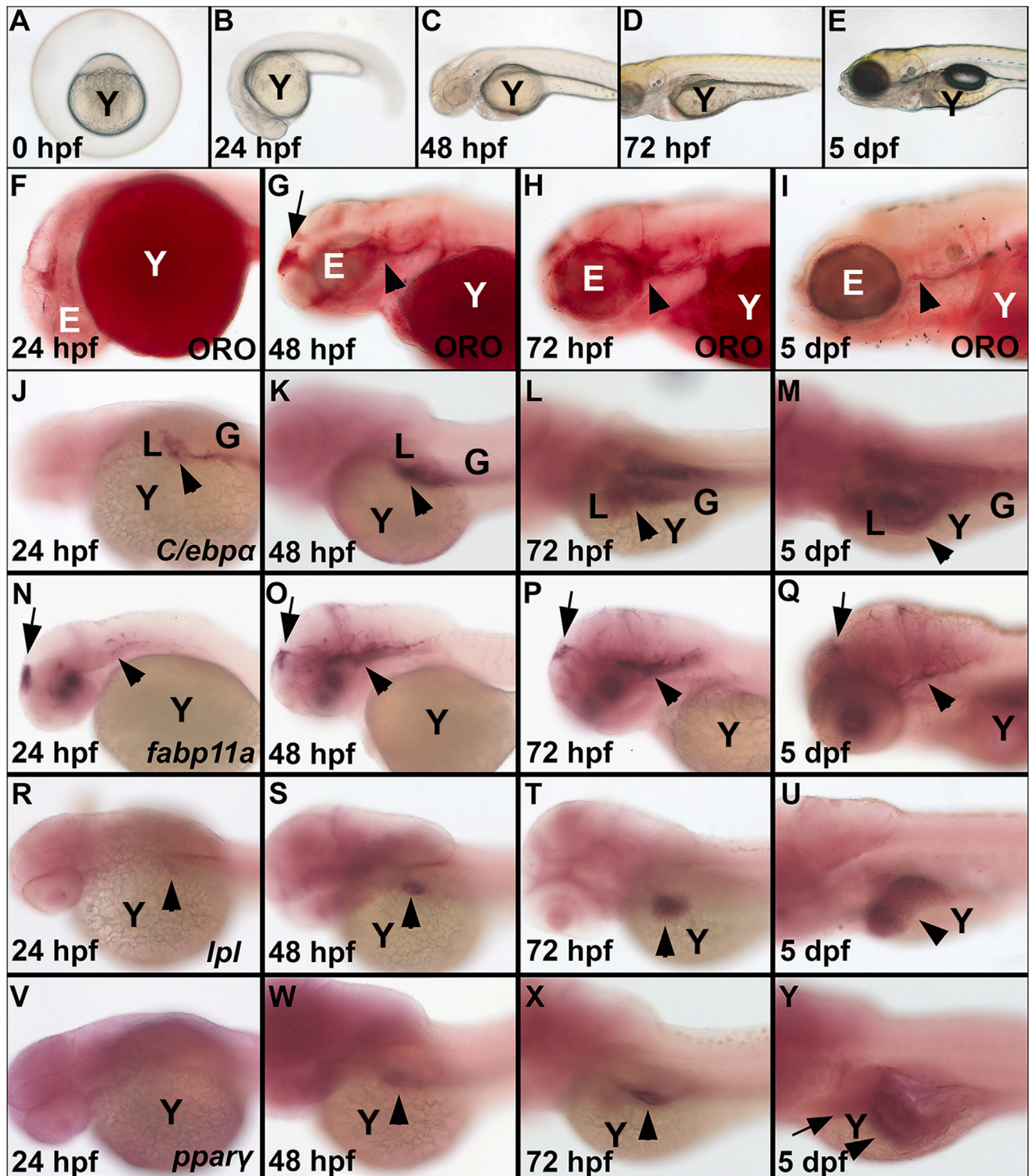
CrossMark

Figure 1. Lipid Distribution and Metabolic Gene Expression throughout Embryogenesis

(A–E) Bright field images show yolk utilization from 0 hpf to 5 dpf.

(F–I) ORO staining shows that there were no deposits of neutral lipid in the head of the embryo at 24 hpf (F), but lipid was present at 48 hpf in the forebrain (arrow, G) and around the eye and underneath the otic vesicle (arrowhead, G), at 72 hpf around the eye (arrowhead, H), and at 5 dpf at a low amount (I).

(J) *c/ebpα* expression was present at 24 hpf in the developing liver and gut (arrowhead).

(K–M) *c/ebpα* expression increased in these organs from 48 hpf to 5 dpf (arrowhead).

(legend continued on next page)

inhibition of key proteins involved in lipid biology (Nishio et al., 2008, 2012).

Additional benefits of the zebrafish as a model are that it develops externally from the mother and embryos undergo discoidal, meroblastic cleavage, a process that separates the developing embryo from the yolk reviewed by Gilbert (2000). This separation is established by a multinucleated cell layer called the yolk syncytial layer (YSL) (Kimmel and Law, 1985) (see Figure S1 for details). These features allow for easy dissociation of the yolk and body of the embryo enabling lipid measurements of the two independently. This provides the opportunity to compare lipid dynamics not only with respect to time, but also between the source (yolk) and its destination (body). Here, we have examined the dynamic properties of lipid molecular species composition, abundance, location, and genetic regulation throughout zebrafish embryogenesis (0–72 hpf) and early larval stages (72–120 hpf). We performed lipidomic analyses to observe changes of 365 individual lipid species, which were grouped into 24 lipid classes and subclasses, within both the yolk and body during zebrafish development. Additionally, we pharmacologically inhibited a crucial nuclear receptor (PPARγ) implicated in lipid metabolism (Ferré, 2004) and studied the changes in lipidomic profile. Furthermore, by using fluorescently labeled lipid analogs BODIPY, we were able to identify the yolk as a site of active lipid metabolism. These analyses have provided an unprecedented examination into the progression of lipidomic composition and metabolism in a developing vertebrate organism revealing active lipid remodeling in the yolk prior to reaching the embryo proper.

RESULTS

Progression of Zebrafish Gene Expression and Lipid Localization during Embryogenesis

Lipidomic analyses were performed at different stages of zebrafish development, at the 1 cell stage or 0 hr post fertilization (hpf) (fertilized embryo, Figure 1A), at 24 hpf, the latest timing of somitogenesis (Figure 1B), during organogenesis at 48 and 72 hpf (Figures 1C and 1D) and during early larval development, soon before zebrafish become free feeding larvae, and at 5 dpf and do not solely rely on yolk reserves anymore (Figure 1E). Note that the size of the yolk contents decreased as embryonic development progressed. Zebrafish were stained with Oil-Red-O (ORO), to label neutral lipids, at the same developmental stages. At 24 hpf, the body was mostly stain-free (Figure 1F). By 48 hpf, stain was present in the forebrain, around the eye, and underneath the otic vesicle (Figure 1G), and increasingly in the vasculature (not shown). At 72 hpf, the stain had increased in these regions and was also detected in the pharyngeal arches, which will later form the gills (Figure 1H). By 5 dpf, the stain decreased throughout the entire body of the embryo, but trace amounts

were still present (Figure 1I). Note that the intensity of ORO staining gradually decreased in the yolk as time progressed, meaning that less neutral lipid was present in the yolk and that most of these lipids had either been used by the embryo or stored in the embryo body. Whole-mount in situ hybridization (WISH) was performed, at the same time points, using mRNA antisense probes for genes that are known to be integral to the activities of lipid metabolism, lipid processing, and lipid mobilization, including the pre-adipocyte marker CCAAT/enhancer-binding protein alpha (*c/ebpα*), the lipid transport protein fatty acid binding protein 11a (*fabp11a*), the lipid processing protein lipoprotein lipase (*lpl*), and a key adipocyte transcription factor peroxisome proliferator-activated receptor gamma (*pparγ*). *c/ebpα* was expressed at 24 hpf in the liver and gut anlage and in the YSL (Figure 1J). Expression continued to increase in these developing organs at all later time points (Figures 1K–1M). Note that in situ hybridization performed using a sense probe for *c/ebpα* or *pparγ* does not stain the developing gut (Figure S1). *fabp11a* was present in the forebrain, in the eye, and in the hindbrain at 24 hpf (Figure 1N). At 48 hpf, the expression increased throughout the head and remained present at these locations at 72 hpf and 5 dpf (Figures 1O–1Q). *lpl* mRNA was located in the liver primordium at 24 hpf (Figure 1R). *lpl* expression gradually increased in the liver as embryogenesis progressed (Figures 1S–1U). *pparγ* was not detected at 24 hpf (Figure 1V). At 48 hpf and 72 hpf, expression was located in the developing gut (Figures 1W–1X). By 5 dpf, *pparγ* expression was strongly detected in the liver, the gut, and swim bladder (Figure 1Y). The evolving and expanding expression patterns of these genes appear to increase throughout development, but also match the initial increase in lipid abundance as detected by ORO.

Temporal Changes of Lipid Classes during Zebrafish Development

In order to discern changes of lipid abundance relative to the yolk and body separately, the two were manually dissected out and analyzed independently (absolute amounts of each lipid species at all time points are listed in Table S1). At 0 hpf, which was considered to be an initial reservoir of lipid for embryonic development, the major lipids present were both polar and non-polar lipids, and in order of decreasing abundance, these were cholesterol (COH), phosphatidylcholine (PC), triacylglycerol (TG), phosphatidylinositol (PI), phosphatidylethanolamine (PE), diacylglycerol (DG), cholesteryl esters (CE), and sphingomyelins (SM) (Figure 2A). Cholesterol was the most abundant at 0 hpf and accounted for 40% of the total lipids, while PCs were 17%, TGs were 9%, PIs were 8%, PEs were 5%, DGs were 4%, CEs were 3%, and SMs were 3%. Other lipid classes that were detected in the yolk sac at lower concentrations included phosphatidylserine (PS), phosphatidylglycerol (PG), the ether linked lipids and plasmalogens, alkylphosphatidylcholine

---

(N–Q) *fabp11a* expression was located in the forebrain (arrow), in the eye and in the hindbrain (arrowhead) from 24 hpf to 5 dpf.
(R–U) *lpl* was present in the developing liver (arrowhead) from 24 to 5 dpf.
(V) *pparγ* was not detected in the embryo at 24 hpf.
(W and X) At 48 and 72 hpf, *pparγ* was expressed in the developing gut (arrowheads).
(Y) At 5 dpf, expression increased in the liver (arrow) and gut (arrowhead) and was present in the swim bladder. E, eye; G, gut; L, liver; Y, yolk.
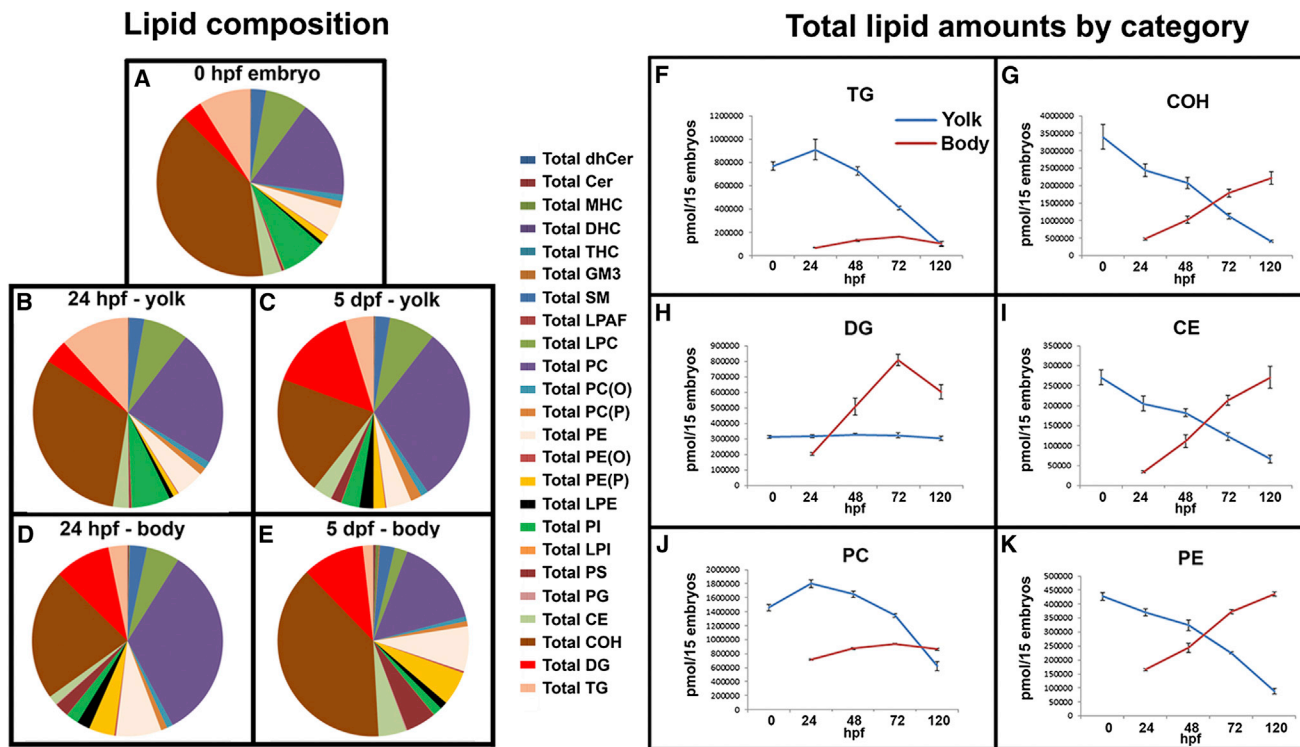See also Figure S1.

Figure 2. Lipid Category Profile of Zebrafish Embryo Yolks and Bodies throughout Embryogenesis

(A–E) The lipid composition of whole zebrafish embryos at 0 hpf (A), of yolks at 24 hpf (B) and 5 dpf (C) and bodies at 24 hpf (D) and 5 dpf (E) are depicted by lipid category percentages relative to the amounts of total lipids detected.

(F–K) Amounts of individual lipid categories for both yolks and bodies are displayed at 0, 24, 48, 72, and 120 hpf for the six most abundant lipid categories: TG (F), COH (G), DG (H), CE (I), PC (J), and PE (K). Lipid species concentrations are shown in pmol/15 embryos.

See also Figure S2 and Table S1.

(PC-O), alkenylphosphatidylcholine (PC-P), alkylphosphatidylethanolamine (PE-O), and alkenylphosphatidylethanolamine (PE-P). We also observed the lysophospholipids, lysophosphatidylethanolamine (LPE), lysophosphatidylcholine (LPC), lysoalkylphosphatidylcholine (LPC-O), and lysophosphatidylinositol (LPI) as well as the sphingolipids, dihydroceramide (dhCer), ceramide (Cer), monohexosylceramide (MHC), dihexosylceramide (DHC), trihexosylceramide (THC), and G_{M3} ganglioside (GM3) (Figure 2A). Most yolk lipids decreased in absolute amounts with increasing days after fertilization, with a majority of those lipids essentially showing a fairly linear decrease. Surprisingly, three lipids showed a rise in concentration between 0 and 24 hpf and then a linear decrease: TG and PC (Figures 2F and 2J) and LPE (Figure S2P). Interestingly, the DG content was maintained at a constant level throughout development (Figure 2H).

In the body, most of the lipid groups referred to for the yolk were present but in low absolute amounts at 24 hpf, with the exception of two of the phospholipids (PC and PE) that were in higher concentration relative to the amount in the yolk at 24 hpf (Figures 2J and 2K). The following body lipids increased in concentration steadily from 24 to 120 hpf: COH, DG, CE, PE, PS, SM, PG, GM3, and dhCer with a slight increase with time for PC (Figures 2G–2K). Relatively low and stable concentrations were detected through time for PI and TG (Figures 2E and 2F). At

5dpf, the four major lipid groups in the body were COH (39%), PC (15%), DG (10%), and PE (8%), while the other lipid classes were present at lower concentrations (Figure 2E). A complete analysis of the concentration of the 24 lipid classes throughout development in both the yolk and the body can be found in Figure S2.

Temporal Dynamics of Lipid Species Composition

When comparing the molecular species showing the highest levels within a class, it was clear there were two distinct patterns: (1) molecular species that were the most abundant within a lipid class, which were the same in the yolk and in the body, and (2) molecular species that were the most abundant within a lipid class, which were not the same in the yolk and in the body as measured by mass spectrometry. Group one consisted of the lipid species PE 40:6, LPE 22:6, PE-O 40:6, PC 34:1, LPAF 16:0, PC-O 38:5, PI 38:6, PS 40:6, PG 16:0-18:1, dhCer 16:0, DHC 16:0, GM3 16:0, SM 34:1, LPC 22:6, and TG 16:0-16:0-18:1. Within group two, the most abundant lipids in the yolk were PE-P 16:0-22:6, PC-P 40:5, Cer 24:1, CE 20:5, MHC 24:1, and DG 16:0-18:1, whereas in the body the most abundant were PE-P 16:0-22:5, PC-P 38:5, Cer 16:0, CE 16:0, MHC 16:0, and DG 16:0-22:6 (not shown).

To reveal the lipid changes during development, the abundance of an individual lipid species was displayed as a relative

change compared to an average level of the specific species across the time intervals, visualized as a heat map. The heat map reveals that most of the lipid species within the yolk sac decreased over time, while most of them increased within the body (Figure S2). It also reveals that many of the TG lipid species reached their highest relative amount at 72 hpf and dropped below the mean at 120 hpf. The same holds true for some DG and PC species (Figure S2). This fits well with our observation that ORO staining was the strongest in the embryos body at 48 and 72 hpf and decreased at 120 hpf (Figures 1G–1I), as ORO stains for neutral lipids including TG. Within the yolk, at the one-cell stage, LPE species 16:1-0:0 and 18:2-0:0 were lower than their mean abundance and they increased to high points at 72 hpf and 120 hpf, respectively. GM3 20:0, 22:0, and 24:0 were not present in the yolk, but were detected in the body. These species rose in a steep linear increase within the body as they were six times, ten times, and 19 times more abundant, respectively, at 120 hpf than they were at 24 hpf. GM3 16:0, which was present in both the yolk and body, increased by 16 times within the body from 24 to 120 hpf (not shown).

Interestingly, not all lipid species decreased within the yolk from 0 to 24 hpf. There were 77 (out of the 332 detected, 23%) lipid species that significantly increased (p < 0.05, using one-way ANOVA and Tukey HSD; see Experimental Procedures) in absolute amount during this developmental period (Table S2). Many of these lipid species were in the TG and PC classes, which showed overall increases in this interval. Notably, TG 18:0-18:0-18:0 increased by more than three times, while TG 14:0-16:0-18:2, 14:0-16:1-18:2, 14:0-18:0-18:1, and 16:1-16:1-16:1 all increased by at least 60% in absolute amount. PC 30:0, 32:2, and 33:0 increased by more than 50% within the yolk from 0 to 24 hpf. Lipid species in classes other than TG and PC increased as well. CE 20:0 increased by 90%. LPC 14:0 increased by more than three times, while LPC 15:0, 18:2, and 20:4 all increased by more than 50%. Cer 20:0 was 57% higher at 24 hpf in the yolk than at 0 hpf. It should be noted that these lipids are present in the yolk at varying relative percentages, and the impact of their increases may depend on their absolute abundances. It is of interest to note that in this period, many of the significant increases were in either saturated or monounsaturated species, the meaning of which is not clear. The trend of increasing lipid species in the yolk did not continue throughout embryonic and larval stages. The increase of lipid species amounts during the first day of development indicates that lipid metabolic processes were occurring in the yolk. However, the number of lipid species that significantly increased during the second day was only seven species.

Fluorescent Lipid Analog Incorporation Reveals a Metabolically Active Yolk Cell

We speculated that the increases in lipids within the yolk were due to an active role of the yolk cell in lipid processing. To confirm this hypothesis, we injected BODIPY-labeled fluorescent lipid analogs into the yolk and followed their incorporation into lipids at different time points post injection. We injected a free fatty acid (FFA) analog, which could be rapidly incorporated into newly synthesized neutral lipids and phospholipids and a PC analog, to mimic endogenous PC metabolism. Embryos were

injected in the center of the yolk cell with approximately 5 nl of a BODIPY analog diluted in olive oil solution (1 mg/ml) at 24 hpf. The injected droplets diffused rapidly, noticeably spreading from the injection droplet by 1 hr post injection (hpi) (Figures 3A and 3D), and continued to diffuse throughout the yolk at later time points, observed up until 6 hpi (Figures 3B and 3E).

Incorporation of lipid analogs was determined by extracting lipids from yolks and embryo bodies separately. Lipid extracts were then run on a thin layer chromatography (TLC) plate and monitored for fluorescent bands. We screened for incorporation at 1 hpi, 3 hpi, and 6 hpi in yolks and bodies (Figures 3C and 3F; see also Figure S3 for non-overplayed plates). In FFA-injected embryos, fluorescence was detected in yolk sample bands that correlated to TG standards as early as 1 hpi (Figure 3C, white arrowheads). Notably, these bands were absent in body samples at 1 hpi and 3 hpi, but a TG band was detected in the embryo body sample at 6 hpi (Figure 3C, asterisk). Additionally, there were bands below these TG bands (Figure 3C, open arrowheads) that followed a similar pattern, in that they were present in yolk samples at each time point and only detected in the bodies at 6 hpi (Figure 3C, pound sign). Furthermore, there were groupings of four bands present in yolk samples at 1 hpi and 3 hpi (Figure 3C, brackets); whereas there was only one band present in the corresponding location in the 1 hpi and 3 hpi body samples (Figure 3C, cross). At 6 hpi, a new band was detected both in the yolk sample and body (Figure 3C, circles).

Newly incorporated fluorescent bands were detected in PC analog injected embryos (Figure 3F). Two bands were present in yolk samples at 1 hpi, 3 hpi, and 6 hpi (Figure 3F, arrows; parentheses) in an area between the FFA and TG lipid standards that were never detected in body samples. Additionally, there was a band present in the yolk samples at all time points (Figure 3F, red arrowheads), which was located close to the position of the DG lipid standard and was not detected in any body samples.

Incorporation of the fluorescent lipid analogs within the yolk, as evidenced by the detection of fluorescent bands, demonstrates that the yolk cell is a site of active lipid metabolism, producing newly formed lipids prior to mobilization into the body. Note that uninjected yolks showed no fluorescent bands (Figure S3). These results explain our observation of increased abundance of some lipid species within the yolk between 0 and 24 hpf (Figures 2, 3, and S2). We concluded from these injection experiments that lipid metabolism is occurring in the yolk prior to mobilization to the body. Our data also demonstrate that different lipids are mobilized at different paces from the yolk to the embryo body. This demonstration that the yolk cell is metabolically active in lipid processing may explain the detection of several lipid metabolizing enzymes in the yolk or YSL throughout development (Table 1; see also Table S3 for list of lipid metabolism gene expressed during zebrafish embryogenesis).

PPARγ Inhibition Modifies Lipid Accumulation in the Developing Embryo

PPARγ is a nuclear receptor transcription factor that is a major component in the development of adipocytes and is highly involved in lipid metabolism (Ferré, 2004; Rosen et al., 1999;
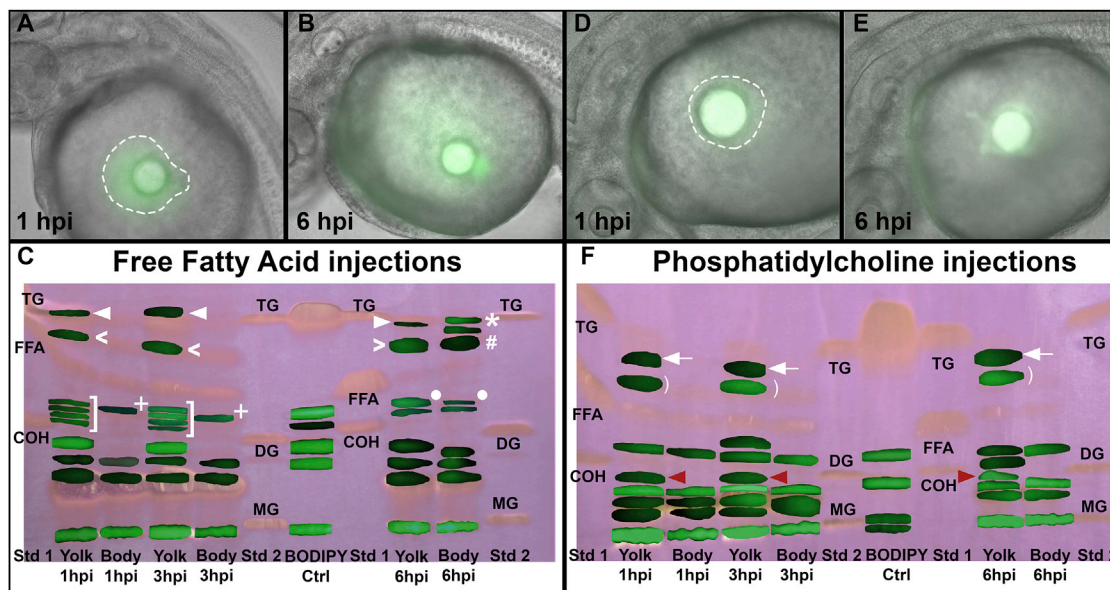
Figure 3. BODIPY-Labeled Lipid Injections Were Incorporated into New Lipids in the Yolk Sac

(A, B, D, and E) BODIPY-labeled FFA and PC were injected into yolk sac of the embryos at 24 hpf. Fluorescent imaging shows spreading of fluorescent FFA (A) and PC (D) at 1 hpi (as marked by dotted white lines) that continued to spread throughout the yolk sac at 6 hpi (B and E).

(C) TLC of BODIPY-labeled FFA injections, with lipid standards in pale orange, shows fluorescent bands in yolk sac samples at 1, 3, and 6 hpi (white arrowheads) and a band at 6 hpi in the body sample (asterisk) that correspond to the TG standard. Bands below the TG bands are present in yolk sac samples at 1, 3, and 6 hpi (open arrowheads) while a similar band is only detected at 6 hpi in the body sample (pound sign). Groupings of four bands, just above the cholesterol standard, were present in yolk samples at 1 hpi and 3 hpi (brackets). One band only was detected in the adjacent area in body samples at 1 hpi and 3 hpi (cross). At 6 hpi, another band is detected above these bands in both the yolk sac and body samples that were not present at earlier time points (circle) demonstrating a temporal dynamic evolution of lipid during development.

(F) TLC of BODIPY-labeled PC injections produced a pair of bands between the TG and FFA standards only in the yolk sac samples at 1, 3, and 6 hpi (arrows, parentheses). These bands were never detected in the body up to 6 hpi. Bands that were located at a level consistent with the DG standard were detected in yolk sac samples at 1, 3, and 6 hpi (red arrowheads) but were never observed in the body up to 6 hpi.

See also Figure S3.

Tontonoz and Spiegelman, 2008). Therefore, we decided to investigate the changes in lipid profile in embryos where PPARγ function had been pharmacologically inactivated. In order to do this, we exposed zebrafish embryos to bisphenol A diglycidyl ether (BADGE) as previously described (Song et al., 2009), which binds to the PPARγ receptor and blocks its activity (Wright et al., 2000). Treatments of zebrafish embryos from 26 hpf to 52 hpf with 5 μM BADGE reduced ORO stain throughout the body of the embryo and notably in the head (Figures 4A and 4B). BADGE exposure also reduced the expression of *c/ebpα* and *lpl* when embryos were treated from 50–72 hpf (Figures 4C–4F). BADGE did not affect the expression of *pparγ* at 72 hpf (Figures 4G and 4H). Inhibiting PPARγ activity was associated with a slight but reproducible increased expression of *fabp11a* in zebrafish embryos (Figures 4I and 4J).

Since we observed decreased ORO stain and expression of *c/ebpα* and *lpl* in BADGE-treated embryos, we wanted to analyze changes that PPARγ inhibition would cause on the lipid profiles of the developing embryos. Therefore, zebrafish embryos were treated with 5 μM BADGE from 26 hpf to 52 hpf, were euthanized, and had the yolks and bodies manually separated (in a similar fashion as presented above). Liquid chromatography (LC)-mass spectrometry was performed on BADGE-treated and control samples to measure the amounts of specific lipid species. The lipidomic analysis revealed that more than one-quarter (25.9%) of lipid species present in control (untreated) bodies were significantly changed in the BADGE-treated bodies (using Tukey HSD). Among the lipid species that were most affected were lysophospholipid species, where PPARγ receptor inhibition increased the concentration of many of the LPCs, LPAFs, and LPEs (Figure 4K). Of the 18 LPCs that were identified, 17 showed an increase of at least 1.48 times the control amount. Five out of the six detected LPAFs were higher than the control (Figure 4K), with the species PC-O 18:0-0:0 at more than two times the amount in the control samples. The dihydroceramides also increased in BADGE-treated embryo bodies, particularly dhCer 18:0, which increased almost eight times compared with control. While most of the phosphatidylcholine species remained unchanged, two species increased significantly; PC 35:4 was almost twice as high and PC 18:2-20:4 was more than 2.5 times higher than the control (Figures 4K and 4L).

In addition to the increases in lipid species, many lipid species decreased in the body in BADGE-treated embryos relative to control amounts. The PC-O and PC-P classes showed a general trend of decreasing. PC-O species 36:5, 38:4, 40:6, and 40:7 all decreased by more than 30% (p < 0.05) compared with the control level, whereas 5 out of the 16 PC-P species analyzed showed

a decrease of at least 25% (p < 0.05). While the PE-O lipids did not show a decrease overall, specific lipid species were noticeably decreased, including PE-O 18:2/18:2 and PE-O 34:1, which were reduced by more than 20% (p = 0.071, p < 0.05 respectively). The PE-P species also had a consistent trend of decreasing. Six out of ten PE-P species showed a significant decrease compared with control (Figures 4K and 4L). For a complete analysis of lipid class changes in BADGE-treated embryos, see Figure S4.

DISCUSSION

In order to provide insight into fundamental lipid properties, we performed lipidomic analysis throughout embryogenesis in a vertebrate organism. To understand the temporal changes in the lipidomic profile of the embryo's body, we measured lipids in the yolk and body separately. This allowed for observation of the dynamic profile of lipids. For example, we observed that the absolute amount of TG amount increased in the yolk from 0 to 24 hpf and then steadily declined. Unexpectedly, in the body, TG only increased a little relative to the amount in yolk (Figure 2F). The low level of TG was probably due to it immediately being used as an energy source upon transfer from the yolk to body. The low relative abundance of TG that we detected in the body at 120 hpf (Figure 2E) fits with a previous report of a relatively low percentage of TG in whole larvae at 6dpf (Miyares et al., 2014).

Measurement of DG revealed a different trend in lipid utilization. Although the amount of DG increased in the body as embryogenesis progressed, a basal level of DG was maintained in the yolk. As DGs are important in cellular signaling (Spiegel et al., 1996), it is possible that maintaining a consistent level of DG is necessary to sustain proper trafficking within the yolk. However, the secondary signaling role of DG may only require low amounts of the lipid and therefore could not account for the quantities that we have observed. DG is an intermediate in the anabolism and catabolism of TG and phospholipids including PC, PE, PI, and PS (Choi et al., 2004; Gibellini and Smith, 2010). Therefore, it is possible that a relatively consistent level of DG is maintained because it was used and produced at the same rate within the processing of metabolic pathways. We noted that while PC increased in absolute amounts in the body from 24 to 120 hpf, it did not increase as sharply as other putative cellular membrane lipids. The level of PC that we detected in the body at 120 hpf, while relatively abundant at 15% of the total lipid (Figure 2E), was not as high as the 32.9% that was reported at 6 dpf (Miyares et al., 2014). This difference was probably due to the PC contained in the yolk that was measured by the latter experiment.

Lipid transport from the yolk to body is poorly understood. Our data reveal a previously unidentified role of the yolk cell in active metabolism of lipids prior to transfer into the body. We measured an increase in nearly one-fourth of lipid species from 0 to 24 hpf (Table S2), including many in TG and PC classes, as well as specific lipids in other classes. Additionally, we observed that exogenous FFA and PC lipid analogs were incorporated into TG and DG lipids, respectively, in the yolk prior to detection in the body. Furthermore, there was incorporation of both analogs into multi-

ple other unidentified lipids. Our gene expression literature search (Table 1) identified that at least three elongations of very long chain fatty acids (elvol) genes are expressed in the yolk or YSL. These elongase enzymes lengthen fatty acids prior to anabolism of more complex lipids (Jakobsson et al., 2006). *Phospholipase A2* and *phospholipase D2* were also found to be expressed in the yolk. Both lipases play roles in processing phospholipids, breaking them down into constituent groups (Jang et al., 2003; Ravaux et al., 2007). These enzymes, along with presumably other metabolic enzymes yet to be found expressing in the yolk, likely act to process the maternally deposited yolk lipids before they are transported into the body. This lipid processing could explain the increases in lipids from 0 to 24 hpf and incorporation of fluorescent lipid analogs within the yolk and demonstrate the yolk cell as a site of metabolic activity.

Further processing and transport of lipids continues in the YSL (Figure S1). Lipids are mobilized to this tissue from granules in the yolk cell, where they can be packaged into lipoproteins and circulated throughout the body (Hölttä-Vuori et al., 2010; Schlegel and Stainier, 2006). By 24 hpf, blood circulation has begun in the zebrafish and is concurrent with the earliest presence of ORO stain that we detected in the vasculature in our embryos. Furthermore, the caudal vein is in direct contact with the YSL at this time (Figure S1). This indicates that circulation may further provide the means to deliver high quantities of lipid throughout the body. Additional lipid transport and processing could occur in the pharynx of the embryo starting around 48 hpf. This structure is located in close proximity to the YSL and yolk (Figure S1). Furthermore, gene expression of adiponectin, the adiponectin receptor, and the leptin receptor in the pharyngeal region has led others to propose that it could play a role in incorporating yolk nutrients into the body (Lampert et al., 2003; Nishio et al., 2008). This idea is supported by the localized expression of phospholipase C, beta 3, phospholipase D1a, high density lipoprotein binding protein a, fatty acid binding protein 3, and several other lipid metabolism-related genes (Table S3). At 4 dpf, lipids have been observed to accumulate in the lumen of the gut (Miyares et al., 2014). Furthermore, by this time, multiple cell types required for digestion are differentiated and present in the intestine (Wallace et al., 2005). It is interesting to speculate that lipids may be processed in the gut before feeding has commenced. By 5 dpf, the yolk has predominantly been used up and the zebrafish begins feeding. Taken together, these data indicate, unlike previously speculated, that the yolk cell is not only a nutrient reserve but it also plays an active role in lipid transformation prior to transport into the embryo's body.

Having developed a comprehensive understanding of the changes in lipid composition in the zebrafish during development, it is now possible to use the model to study various aspects of lipid metabolism and its regulation. We postulated that inhibition of PPARγ would cause a change in the lipid profile of the embryo as PPARγ is highly involved in adipogenesis (Rosen et al., 1999). A notable effect of BADGE treatment on the embryos was an increase in lysophospholipid species. In a previous study, a PPARγ chemical agonist was shown to decrease the mRNA expression and activity of phospholipase A2 in cultured rat vascular smooth muscle cells

Table 1. Lipid-Associated Genes Expressed in the Yolk of Zebrafish

Gene Name (Zebrafish Gene Abbreviation)	Known Function	Timing of Expression in Zebrafish	References
Phospholipase A2, group XIIB (pla2g12b)	phospholipase A2 enzymes hydrolyze ester bonds of glyceroacylphospholipids to produce lysophospholipids and nonesterified fatty acids (Ravaux et al., 2007)	50% epiboly-5 dpf	Thisse and Thisse, 2004
Phospholipase B domain containing 1 (plbd1)	unknown	50% epiboly-60 hpf	Thisse and Thisse, 2004
Phospholipase D2 (pld2)	phospholipase D hydrolyzes phosphatidylcholine to generate phosphatidic acid (PA) and choline (Jang et al., 2003)	50% epiboly-10 hpf, 4–13 dpf	Liu et al., 2010; Thisse and Thisse, 2004
Patatin-like phospholipase domain containing 7b (pnpla7b)	unknown	one cell-72 hpf	Thisse and Thisse, 2004
Apolipoprotein A-Ia (apoA-Ia)	apolipoprotein A-I is the major protein component of high density lipoprotein in plasma (Schonfeld and Pfleger, 1974)	6 hpf-72 hpf, adult	Babin et al., 1997; Thisse et al., 2001
Apolipoprotein A-II (apoA-II)	apolipoprotein A-II is the second most abundant protein of the high density lipoprotein particles (Schonfeld et al., 1977)	four cell-72 hpf, adult	Thisse et al., 2001; Cheng et al., 2006; Zhang et al., 2011
Apolipoprotein A-IVa (apoA-IVa)	apolipoprotein A-IV is a key protein component of chylomicrons (Wang et al., 2013)	50% epiboly-60 hpf	Thisse and Thisse, 2004
Apolipoprotein A-IV b, tandem duplicate 1 (apoA-IVb.1)		50% epiboly-5 dpf, adult	Thisse and Thisse, 2004; Levi et al., 2012
Apolipoprotein A-IV b, tandem duplicate 2 (apoA-IVb.2)		two cell-5 dpf	Rauch et al., 2003
Apolipoprotein Ba (apoBa)	apolipoprotein B is the primary apolipoprotein of chylomicrons and low-density lipoproteins (Kane et al., 1980; Knott et al., 1986)	50% epiboly-60 hpf, adult	Thisse and Thisse, 2004; Cheng et al., 2006
Apolipoprotein Bb, tandem duplicate 1 (apoBb.1)		50% epiboly-60 hpf, adult	Thisse and Thisse, 2004
Apolipoprotein Ea (apoEa)	apolipoprotein E is a class of apolipoprotein found in the chylomicron and LDLs. It is important in lipoprotein receptor binding (Mahley, 1988)	50% epiboly-60 hpf	Thisse and Thisse, 2004
Apolipoprotein Eb (apoEb)		128 cell-5 dpf, adult	Thisse and Thisse, 2005
Microsomal triglyceride transfer protein (mtp)	MTP combines TG, cholesterol esters of fatty acids, free cholesterol, and phospholipids with apolipoprotein B to form chylomicrons (Schlegel and Stainier, 2006)	one cell-5 dpf, adult	Thisse and Thisse, 2004; Marza et al., 2005
ELOVL fatty acid elongase 2 (elovl2)	ELOVLs are involved in fatty acid synthesis by elongating fatty acid chains (Jakobsson et al., 2006)	one cell-5 dpf, adult	Monroig et al., 2009
ELOVL fatty acid elongase 5 (elovl5)		one cell-60 hpf, adult	Thisse and Thisse, 2004; Monroig et al., 2009
ELOVL fatty acid elongase 6 (elovl6)		50% epiboly-60 hpf	Thisse and Thisse, 2004
Fatty acid binding protein 1b, tandem duplicate 1 (fabp1b.1)	fatty acid binding proteins regulate fatty acid transport (Chmurzyńska, 2006)	10 hpf-5 dpf, adult	Sharma et al., 2006
24-Dehydrocholesterol reductase (dhcr24)	DHCR24 is an oxidoreductase that catalyzes the reduction of the delta-24 double bond of sterol intermediates during cholesterol biosynthesis (Waterham et al., 2001)	50% epiboly-60 hpf	Thisse and Thisse, 2004
Delta(4)-desaturase, sphingolipid 1 (degs1)	DEGS1 converts dhCer into Cer (Ruangsiriluk et al., 2012)	50% epiboly-60 hpf	Thisse and Thisse, 2004

Table 1. *Continued*

Gene Name (Zebrafish Gene Abbreviation)	Known Function	Timing of Expression in Zebrafish	References
Arylsulfatase A (arsa)	arylsulfatase A is an enzyme that hydrolyzes the sulfate ester bond of cerebroside 3-sulfate, a component of the myelin sheath, to produce cerebroside and sulfate (Lukatela et al., 1998)	one cell-72 hpf	Thisse and Thisse, 2004
Sphingomyelin phosphodiesterase 2a (smpd2a)	SMPD2 is responsible for breaking sphingomyelin down into phosphocholine and ceramide (Ago et al., 2006)	50% epiboly-60 hpf	Thisse and Thisse, 2004
Acyl-CoA synthetase long-chain family member 4a (acsl4a)	ACSL enzymes convert free fatty acids to fatty acyl-CoAs as the initial step in a majority of processing events (Miyares et al., 2014)	four cell-4 dpf	Miyares et al., 2014
Acyl-CoA synthetase long-chain family member 4b (acsl4b)		50% epiboly-60 hpf	Thisse and Thisse, 2004
Enoyl-CoA, hydratase/3-hydroxyacyl-CoA dehydrogenase (ehhadh)	this enzyme catalyzes the metabolism of fatty acids to produce acetyl-CoA and energy (Bahnson et al., 2002)	one cell-72 hpf, adult	Thisse and Thisse, 2004
Acyl-CoA synthetase long-chain family member 1b (acsl1b)	all ACSLs convert long-chain fatty acids into acyl-CoA (Soupene and Kuypers, 2008)	50% epiboly-60 hpf	Thisse and Thisse, 2004
Acyl-CoA synthetase long-chain family member 5 (acsl5)		one cell-60 hpf	Thisse and Thisse, 2004
ATP-binding cassette transporter (abca1b)	ABCA1 is a cholesterol and phospholipid transporter in conjunction with Apolipoprotein A-I (Wang et al., 2001)	50% epiboly-5 dpf	Thisse and Thisse, 2004
Scavenger receptor class b, member 1 (scarb1)	SCARB1 acts as a receptor for HDL and may influence its plasma levels (Rigotti et al., 1997)	50% epiboly-19 hpf	Thisse and Thisse, 2004
Cholesteryl ester transfer protein (cetp)	CETP is an enzyme that mediates the exchange of lipids between lipoproteins (Kuivenhoven et al., 1998)	50% epiboly-5 dpf	Thisse and Thisse, 2004
ORMDL sphingolipid biosynthesis regulator 3 (ormdl3)	ORMDL3 may regulate ceramide biosynthesis, but its function is still unknown (Siow and Wattenberg, 2012)	one cell-72 hpf	Thisse and Thisse, 2004

List of genes expressed in the yolk sac, their know function, and their timing of expression.
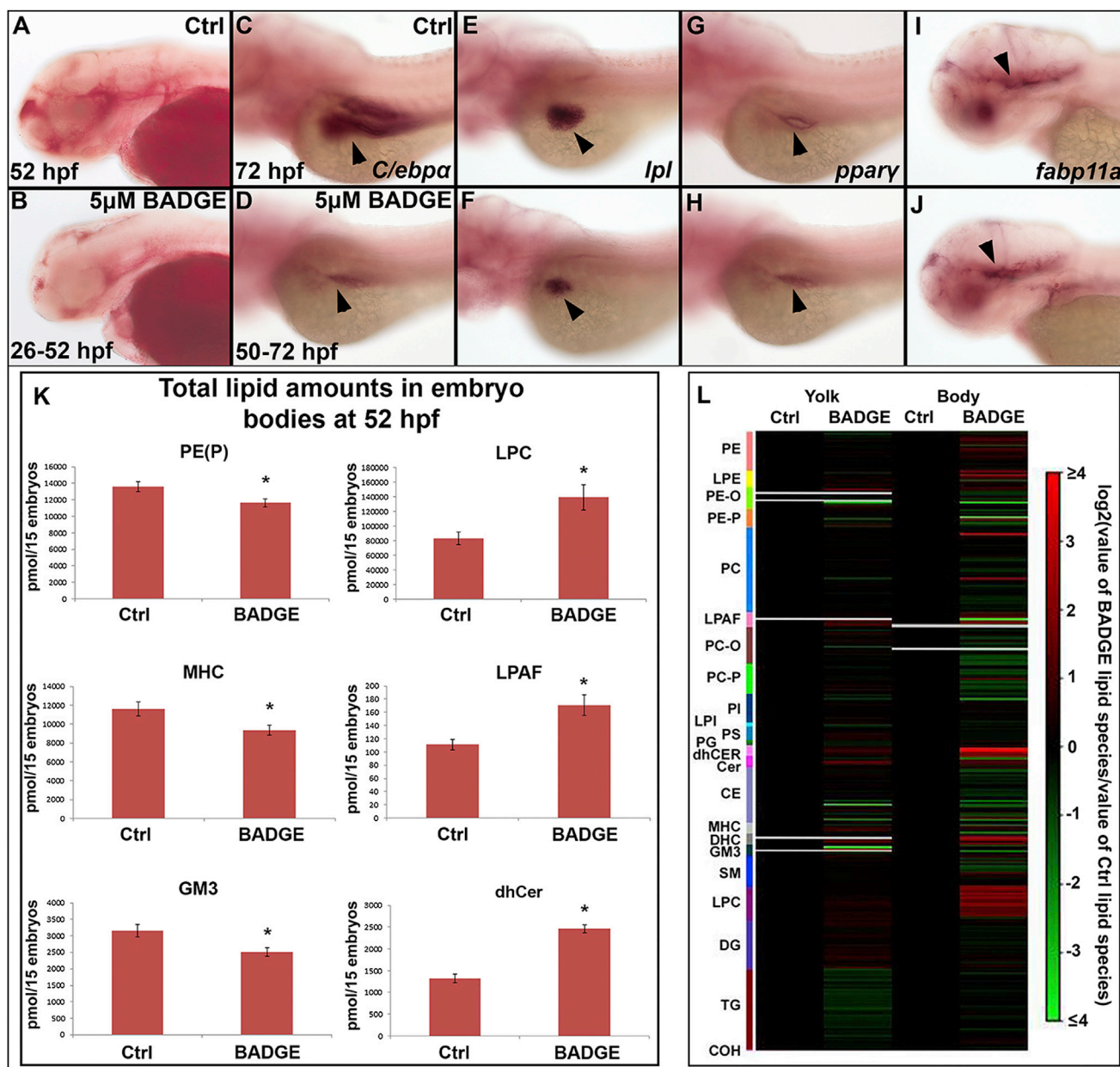See also Tables S2 and S3.

Figure 4. The Effects of PPARγ Inhibition on the Lipid Profile and Gene Expression of Zebrafish Embryos

(A and B) ORO staining showed decreased lipid present in embryos treated with 5 μM BADGE from 26–52 hpf (B) compared with controls (A).

(C–J) Treatment with 5 μM BADGE from 50–72 hpf decreased the expression of *c/ebpα* (C and D, arrowheads) and *lpl* (E and F, arrowheads), did not affect the expression of *pparγ* (G and H, arrowheads) and increased the expression of *fabp11a* (I and J, arrowheads).

(K) Lipid amounts are depicted for lipid categories that were significantly changed by exposure to 5 μM BADGE from 26–52 hpf. Lipid species concentrations are shown in pmol/15 embryos (K). The amount of each individual lipid at a single time point in 5 μM BADGE-treated embryos was set relative to the level of that lipid species in control embryos. *p < 0.05.

(L) A log2 ratio was then calculated for the signals of each lipid species. Red indicates an increase compared to the mean, green indicates a decrease and black shows no change. Gray is displayed when there is no lipid present.

See also Figure S4.

(Ravaux et al., 2007). Phospholipase A2 is responsible for producing lysophospholipid species from phospholipids (D'Arrigo and Servi, 2010). Therefore, it is reasonable to presume that in our PPARγ-inhibited embryos there may have been an increase in phospholipase A2 expression and activity that could have the led to the increased levels of the lysophospholipid species. Although the lysophospholipid data correlated to results reported in a previous study (Ravaux et al., 2007), many

additional changes in the lipids in the BADGE-treated embryos were identified in this project. Liquid chromatography-mass spectrometry provides a promising tool for in depth analyses into many aspects of lipid biology, including pharmacological, disease, or metabolic studies, in an amenable model organism.

EXPERIMENTAL PROCEDURES

Lipid Extraction

Lipids were extracted with dichloromethane:methanol (2:1) using the Folch method (Folch et al., 1957). The organic phase was dried with nitrogen and reconstituted in 50 μl of chloroform for thin layer chromatography (TLC).

Thin Layer Chromatography

Samples were run on silica gel 60 aluminum sheets (Merck Millipore). Twenty-five microliters of samples and standards were spotted on the plate. TLC plates were developed in a solution of 43 ml petroleum ether, 7 ml diethyl ether, and 1 ml acetic acid. Standard 1 (Nu-chek Prep) contains equal parts lecithin (1,2 distearoyl), cholesterol, oleic acid, triolein, and cholesteryl oleate. Standard 2 (Nu-chek Prep) contains equal parts monoolein, diolein, triolein, and methyl oleate. Positive controls were 0.5 μl BODIPY/oil stock dissolved in 25 μl of chloroform. Non-fluorescent lipids were detected with $KMnO_4$ stain giving a pale orange color.

For complete experimental procedures, see the Supplemental Information.

SUPPLEMENTAL INFORMATION

Supplemental Information includes Supplemental Experimental Procedures, four figures, and three tables and can be found with this article online at http://dx.doi.org/10.1016/j.celrep.2016.01.016.

AUTHOR CONTRIBUTIONS

D.F. performed zebrafish experimental work and lipidomics works, image acquisition, data quantification, and data analysis. A.S. performed data quantification and data analysis. N.A.M. and P.J.M. performed lipidomics work. A.J.S. and Y.G. designed the experiments. D.F., A.J.S., and Y.G. wrote the paper. Y.G. directed the research.

ACKNOWLEDGMENTS

REFERENCES

Ago, H., Oda, M., Takahashi, M., Tsuge, H., Ochi, S., Katunuma, N., Miyano, M., and Sakurai, J. (2006). Structural basis of the sphingomyelin phosphodiesterase activity in neutral sphingomyelinase from Bacillus cereus. J. Biol. Chem. 281, 16157–16167.

Allen, J.D., and Pernet, B. (2007). Intermediate modes of larval development: bridging the gap between planktotrophy and lecithotrophy. Evol. Dev. 9, 643–653.

Babin, P.J., Thisse, C., Durliat, M., Andre, M., Akimenko, M.-A., and Thisse, B. (1997). Both apolipoprotein E and A-I genes are present in a nonmammalian vertebrate and are highly expressed during embryonic development. Proc. Natl. Acad. Sci. USA 94, 8622–8627.

Bahnson, B.J., Anderson, V.E., and Petsko, G.A. (2002). Structural mechanism of enoyl-CoA hydratase: three atoms from a single water are added in either an E1cb stepwise or concerted fashion. Biochemistry 41, 2621–2629.

Belkhou, R., Cherel, Y., Heitz, A., Robin, J.-P., and Le Maho, Y. (1991). Energy contribution of proteins and lipids during prolonged fasting in the rat. Nutr. Res. 11, 365–374.

Carten, J.D., Bradford, M.K., and Farber, S.A. (2011). Visualizing digestive organ morphology and function using differential fatty acid metabolism in live zebrafish. Dev. Biol. 360, 276–285.

Cheng, W., Guo, L., Zhang, Z., Soo, H.M., Wen, C., Wu, W., and Peng, J. (2006). HNF factors form a network to regulate liver-enriched genes in zebrafish. Dev. Biol. 294, 482–496.

Chmurzyńska, A. (2006). The multigene family of fatty acid-binding proteins (FABPs): function, structure and polymorphism. J. Appl. Genet. 47, 39–48.

Choi, H.-S., Sreenivas, A., Han, G.-S., and Carman, G.M. (2004). Regulation of phospholipid synthesis in the yeast cki1Δ eki1Δ mutant defective in the Kennedy pathway. The Cho1-encoded phosphatidylserine synthase is regulated by mRNA stability. J. Biol. Chem. 279, 12081–12087.

D'Arrigo, P., and Servi, S. (2010). Synthesis of lysophospholipids. Molecules 15, 1354–1377.

Dawid, I.B. (2004). Developmental biology of zebrafish. Ann. N Y Acad. Sci. 1038, 88–93.

Fang, L., Liu, C., and Miller, Y.I. (2014). Zebrafish models of dyslipidemia: relevance to atherosclerosis and angiogenesis. Transl. Res. 163, 99–108.

Ferré, P. (2004). The biology of peroxisome proliferator-activated receptors: relationship with lipid metabolism and insulin sensitivity. Diabetes 53 (Suppl 1), S43–S50.

Ferreira, C.R., Saraiva, S.A., Catharino, R.R., Garcia, J.S., Gozzo, F.C., Sanvido, G.B., Santos, L.F.A., Lo Turco, E.G., Pontes, J.H.F., Basso, A.C., et al. (2010). Single embryo and oocyte lipid fingerprinting by mass spectrometry. J. Lipid Res. 51, 1218–1227.

Folch, J., Lees, M., and Sloane Stanley, G.H. (1957). A simple method for the isolation and purification of total lipides from animal tissues. J. Biol. Chem. 226, 497–509.

Flynn, E.J., 3rd, Trent, C.M., and Rawls, J.F. (2009). Ontogeny and nutritional control of adipogenesis in zebrafish (Danio rerio). J. Lipid Res. 50, 1641–1652.

Gibellini, F., and Smith, T.K. (2010). The Kennedy pathway–De novo synthesis of phosphatidylethanolamine and phosphatidylcholine. IUBMB Life 62, 414–428.

Gilbert, S.F. (2000). Early development in fish. In Developmental Biology (Sinauer Associates).

González-Serrano, A.F., Pirro, V., Ferreira, C.R., Oliveri, P., Eberlin, L.S., Heinzmann, J., Lucas-Hahn, A., Niemann, H., and Cooks, R.G. (2013). Desorption electrospray ionization mass spectrometry reveals lipid metabolism of individual oocytes and embryos. PLoS ONE 8, e74981.

Guan, X.L., Cestra, G., Shui, G., Kuhrs, A., Schittenhelm, R.B., Hafen, E., van der Goot, F.G., Robinett, C.C., Gatti, M., Gonzalez-Gaitan, M., and Wenk, M.R. (2013). Biochemical membrane lipidomics during Drosophila development. Dev. Cell 24, 98–111.

Heras, H., Gonzalez-Baró, M.R., and Pollero, R.J. (2000). Lipid and fatty acid composition and energy partitioning during embryo development in the shrimp Macrobrachium borellii. Lipids 35, 645–651.

Hölttä-Vuori, M., Salo, V.T., Nyberg, L., Brackmann, C., Enejder, A., Panula, P., and Ikonen, E. (2010). Zebrafish: gaining popularity in lipid research. Biochem. J. 429, 235–242.

Jakobsson, A., Westerberg, R., and Jacobsson, A. (2006). Fatty acid elongases in mammals: their regulation and roles in metabolism. Prog. Lipid Res. 45, 237–249.

Jang, I.H., Lee, S., Park, J.B., Kim, J.H., Lee, C.S., Hur, E.-M., Kim, I.S., Kim, K.-T., Yagisawa, H., Suh, P.-G., and Ryu, S.H. (2003). The direct interaction of phospholipase C-γ 1 with phospholipase D2 is important for epidermal growth factor signaling. J. Biol. Chem. 278, 18184–18190.

Kane, J.P., Hardman, D.A., and Paulus, H.E. (1980). Heterogeneity of apolipoprotein B: isolation of a new species from human chylomicrons. Proc. Natl. Acad. Sci. USA 77, 2465–2469.

Kimmel, C.B., and Law, R.D. (1985). Cell lineage of zebrafish blastomeres. II. Formation of the yolk syncytial layer. Dev. Biol. 108, 86–93.

Knott, T.J., Pease, R.J., Powell, L.M., Wallis, S.C., Rall, S.C., Jr., Innerarity, T.L., Blackhart, B., Taylor, W.H., Marcel, Y., Milne, R., et al. (1986). Complete protein sequence and identification of structural domains of human apolipoprotein B. Nature 323, 734–738.

Kuivenhoven, J.A., Jukema, J.W., Zwinderman, A.H., de Knijff, P., McPherson, R., Bruschke, A.V., Lie, K.I., and Kastelein, J.J.; The Regression Growth Evaluation Statin Study Group (1998). The role of a common variant of the cholesteryl ester transfer protein gene in the progression of coronary atherosclerosis. N. Engl. J. Med. 338, 86–93.

Kunz-Ramsay, Y. (2013). Lecithotrophic species. In Developmental Biology of Teleost Fishes (Springer Science & Business Media).

Lampert, J.M., Holzschuh, J., Hessel, S., Driever, W., Vogt, K., and von Lintig, J. (2003). Provitamin A conversion to retinal via the β,β-carotene-15,15′-oxygenase (bcox) is essential for pattern formation and differentiation during zebrafish embryogenesis. Development 130, 2173–2186.

Levi, L., Ziv, T., Admon, A., Levavi-Sivan, B., and Lubzens, E. (2012). Insight into molecular pathways of retinal metabolism, associated with vitellogenesis in zebrafish. Am. J. Physiol. Endocrinol. Metab. 302, E626–E644.

Liu, H.-Y., Lee, N., Tsai, T.-Y., and Ho, S.-Y. (2010). Zebrafish fat-free, a novel Arf effector, regulates phospholipase D to mediate lipid and glucose metabolism. Biochim. Biophys. Acta 1801, 1330–1340.

Lukatela, G., Krauss, N., Theis, K., Selmer, T., Gieselmann, V., von Figura, K., and Saenger, W. (1998). Crystal structure of human arylsulfatase A: the aldehyde function and the metal ion at the active site suggest a novel mechanism for sulfate ester hydrolysis. Biochemistry 37, 3654–3664.

Mahley, R.W. (1988). Apolipoprotein E: cholesterol transport protein with expanding role in cell biology. Science 240, 622–630.

Marza, E., Barthe, C., André, M., Villeneuve, L., Hélou, C., and Babin, P.J. (2005). Developmental expression and nutritional regulation of a zebrafish gene homologous to mammalian microsomal triglyceride transfer protein large subunit. Dev. Dyn. 232, 506–518.

Miyares, R.L., de Rezende, V.B., and Farber, S.A. (2014). Zebrafish yolk lipid processing: a tractable tool for the study of vertebrate lipid transport and metabolism. Dis. Model. Mech. 7, 915–927.

Monroig, O., Rotllant, J., Sánchez, E., Cerdá-Reverter, J.M., and Tocher, D.R. (2009). Expression of long-chain polyunsaturated fatty acid (LC-PUFA) biosynthesis genes during zebrafish Danio rerio early embryogenesis. Biochim. Biophys. Acta 1791, 1093–1101.

Nishio, S., Gibert, Y., Bernard, L., Brunet, F., Triqueneaux, G., and Laudet, V. (2008). Adiponectin and adiponectin receptor genes are coexpressed during zebrafish embryogenesis and regulated by food deprivation. Dev. Dyn. 237, 1682–1690.

Nishio, S., Gibert, Y., Berekelya, L., Bernard, L., Brunet, F., Guillot, E., Le Bail, J.-C., Sánchez, J.A., Galzin, A.M., Triqueneaux, G., and Laudet, V. (2012). Fasting induces CART down-regulation in the zebrafish nervous system in a cannabinoid receptor 1-dependent manner. Mol. Endocrinol. 26, 1316–1326.

Rauch, G., Lyons, D., Middendorf, I., Friedlander, B., Arana, N., Reyes, T., and Talbot, W. (2003). Submission and curation of gene expression data. ZFIN Direct Data Submission (http://zfin.org).

Ravaux, L., Denoyelle, C., Monne, C., Limon, I., Raymondjean, M., and El Hadri, K. (2007). Inhibition of interleukin-1β-induced group IIA secretory phospholipase A2 expression by peroxisome proliferator-activated receptors (PPARs) in rat vascular smooth muscle cells: cooperation between PPARbeta and the proto-oncogene BCL-6. Mol. Cell. Biol. 27, 8374–8387.

Rigotti, A., Trigatti, B.L., Penman, M., Rayburn, H., Herz, J., and Krieger, M. (1997). A targeted mutation in the murine gene encoding the high density lipoprotein (HDL) receptor scavenger receptor class B type I reveals its key role in HDL metabolism. Proc. Natl. Acad. Sci. USA 94, 12610–12615.

Rosa, R., Calado, R., Andrade, A.M., Narciso, L., and Nunes, M.L. (2005). Changes in amino acids and lipids during embryogenesis of European lobster, Homarus gammarus (Crustacea: Decapoda). Comp. Biochem. Physiol. B Biochem. Mol. Biol. 140, 241–249.

Rosen, E.D., Sarraf, P., Troy, A.E., Bradwin, G., Moore, K., Milstone, D.S., Spiegelman, B.M., and Mortensen, R.M. (1999). PPAR γ is required for the differentiation of adipose tissue in vivo and in vitro. Mol. Cell 4, 611–617.

Ruangsiriluk, W., Grosskurth, S.E., Ziemek, D., Kuhn, M., des Etages, S.G., and Francone, O.L. (2012). Silencing of enzymes involved in ceramide biosynthesis causes distinct global alterations of lipid homeostasis and gene expression. J. Lipid Res. 53, 1459–1471.

Schlegel, A. (2012). Studying non-alcoholic fatty liver disease with zebrafish: a confluence of optics, genetics, and physiology. Cell. Mol. Life Sci. 69, 3953–3961.

Schlegel, A., and Gut, P. (2015). Metabolic insights from zebrafish genetics, physiology, and chemical biology. Cell. Mol. Life Sci. 72, 2249–2260.

Schlegel, A., and Stainier, D.Y. (2006). Microsomal triglyceride transfer protein is required for yolk lipid utilization and absorption of dietary lipids in zebrafish larvae. Biochemistry 45, 15179–15187.

Schonfeld, G., and Pfleger, B. (1974). The structure of human high density lipoprotein and the levels of apolipoprotein A-I in plasma as determined by radioimmunoassay. J. Clin. Invest. 54, 236–246.

Schonfeld, G., Chen, J., McDonnell, W.F., and Jeng, I. (1977). Apolipoprotein A-II content of human plasma high density lipoproteins measured by radioimmunoassay. J. Lipid Res. 18, 645–655.

Sharma, M.K., Liu, R.Z., Thisse, C., Thisse, B., Denovan-Wright, E.M., and Wright, J.M. (2006). Hierarchical subfunctionalization of fabp1a, fabp1b and fabp10 tissue-specific expression may account for retention of these duplicated genes in the zebrafish (Danio rerio) genome. FEBS J. 273, 3216–3229.

Simons, K., and Ikonen, E. (1997). Functional rafts in cell membranes. Nature 387, 569–572.

Siow, D.L., and Wattenberg, B.W. (2012). Mammalian ORMDL proteins mediate the feedback response in ceramide biosynthesis. J. Biol. Chem. 287, 40198–40204.

Song, Y., Selak, M.A., Watson, C.T., Coutts, C., Scherer, P.C., Panzer, J.A., Gibbs, S., Scott, M.O., Willer, G., Gregg, R.G., et al. (2009). Mechanisms underlying metabolic and neural defects in zebrafish and human multiple acyl-CoA dehydrogenase deficiency (MADD). PLoS ONE 4, e8329.

Soupene, E., and Kuypers, F.A. (2008). Mammalian long-chain acyl-CoA synthetases. Exp. Biol. Med. (Maywood) 233, 507–521.

Spiegel, S., Foster, D., and Kolesnick, R. (1996). Signal transduction through lipid second messengers. Curr. Opin. Cell Biol. 8, 159–167.

Thisse, B., and Thisse, C. (2004). Fast release clones: a high throughput expression analysis. ZFIN Direct Data Submission (http://zfin.org).

Thisse, C., and Thisse, B. (2005). High throughput expression analysis of ZF-models consortium clones. ZFIN Direct Data Submission (http://zfin.org).

Thisse, B., Pflumio, S., Fürthauer, M., Loppin, B., Heyer, V., Degrave, A., Woehl, R., Lux, A., Steffan, T., and Charbonnier, X. (2001). Expression of the zebrafish genome during embryogenesis. ZFIN Direct Data Submission (http://zfin.org).

Tontonoz, P., and Spiegelman, B.M. (2008). Fat and beyond: the diverse biology of PPARgamma. Annu. Rev. Biochem. 77, 289–312.

Wallace, K.N., Akhter, S., Smith, E.M., Lorent, K., and Pack, M. (2005). Intestinal growth and differentiation in zebrafish. Mech. Dev. 122, 157–173.

Wang, N., Silver, D.L., Thiele, C., and Tall, A.R. (2001). ATP-binding cassette transporter A1 (ABCA1) functions as a cholesterol efflux regulatory protein. J. Biol. Chem. 276, 23742–23747.

Wang, F., Pearson, K.J., Davidson, W.S., and Tso, P. (2013). Specific sequences in N termini of apolipoprotein A-IV modulate its anorectic effect. Physiol. Behav. 120, 136–142.

Waterham, H.R., Koster, J., Romeijn, G.J., Hennekam, R.C., Vreken, P., Andersson, H.C., FitzPatrick, D.R., Kelley, R.I., and Wanders, R.J. (2001).

Mutations in the 3β-hydroxysterol Δ24-reductase gene cause desmosterolosis, an autosomal recessive disorder of cholesterol biosynthesis. Am. J. Hum. Genet. *69*, 685–694.

Wiegand, M.D. (1996). Composition, accumulation and utilization of yolk lipids in teleost fish. Rev. Fish Biol. Fish. *6*, 259–286.

Wright, H.M., Clish, C.B., Mikami, T., Hauser, S., Yanagi, K., Hiramatsu, R., Serhan, C.N., and Spiegelman, B.M. (2000). A synthetic antagonist for the peroxisome proliferator-activated receptor γ inhibits adipocyte differentiation. J. Biol. Chem. *275*, 1873–1877.

Zhang, T., Yao, S., Wang, P., Yin, C., Xiao, C., Qian, M., Liu, D., Zheng, L., Meng, W., Zhu, H., et al. (2011). ApoA-II directs morphogenetic movements of zebrafish embryo by preventing chromosome fusion during nuclear division in yolk syncytial layer. J. Biol. Chem. *286*, 9514–9525.

Zon, L.I. (1999). Zebrafish: a new model for human disease. Genome Res. *9*, 99–100.